63-3-6

ARL 63-48

AUTOMATIC OPTICAL RANGE FINDER

WERNER RAMBAUSKE
HUBERT KUESTERS

FEBRUARY 1963

AERONAUTICAL RESEARCH LABORATORIES
OFFICE OF AEROSPACE RESEARCH
UNITED STATES AIR FORCE

NOTICES

When Government drawings, specifications, or other data are used for any purpose other than in connection with a definitely related Government procurement operation, the United States Government thereby incurs no responsibility nor any obligation whatsoever; and the fact that the Government may have formulated, furnished, or in any way supplied the said drawings, specifications, or other data, is not to be regarded by implication or otherwise as in any manner licensing the holder or any other person or corporation, or conveying any rights or permission to manufacture, use, or sell any patented invention that may in any way be related thereto.

- - - - - - - - - -

Qualified requesters may obtain copies of this report from the Armed Services Technical Information Agency, (ASTIA), Arlington Hall Station, Arlington 12, Virginia.

- - - - - - - - - -

This report has been released to the Office of Technical Services, U. S. Department of Commerce, Washington 25, D. C. for sale to the general public.

- - - - - - - - - -

Copies of ARL Technical Documentary Reports should not be returned to Aeronautical Research Laboratory unless return is required by security considerations, contractual obligations, or notices on a specific document.

11-791, 400, 6-14-61

ARL 63-48

AUTOMATIC OPTICAL RANGE FINDER

WERNER RAMBAUSKE
HUBERT KUESTERS

FEBRUARY 1963

PROJECT 7072
TASK 70827

AERONAUTICAL RESEARCH LABORATORIES
OFFICE OF AEROSPACE RESEARCH
UNITED STATES AIR FORCE
WRIGHT-PATTERSON AIR FORCE BASE, OHIO

FOREWORD

This technical report was accomplished under Project RDO No. 466-3-1, High Speed Optical Comparator, Project 7072, Research on Quantum Nature of Light, and Task 70827, Light Amplification. The bulk of the experimental work was performed under the direction of Dr. John E. Clemens and guidance of Dr. Ben B. Johnstone. Their contributions and support which made the endeavor possible are herewith acknowledged. The basic idea of the reported multisensor opto-electronic range finder system, which compensates for an extended target was conceived by Dr. Werner Rambauske. Acknowledgement is also given to the other members of the team working and consulting with the authors on the task:

Radames K.H. Gebel, Electronics

Rudolf Opitz, Optics

Richard Orthuber, Acquisition and Detection

and Raymond Roth, Measurements

This report was not released at an earlier date because of previous classification.

Abstract

The different possible conventional methods usable for passive electronic range finding are analyzed. A new method is suggested, having considerable advantages over these. A working model to demonstrate this new method was designed and built for evaluation of experimental data and detailed descriptions are added to the report.

CONTENTS

LIST OF FIGURES

LIST OF FIGURES (Cont.)

I. INTRODUCTION

Rangefinding is either of active or of passive nature. In active rangefinders, radiation is emitted from a radiation source at the locations of the observer. In passive rangefinders, the natural emission and/or reflection of radiation of the target, or the difference of the target emission or reflection to background emission or reflection (scattering) are utilized.

The system described in this report deals with the passive rangefinding and is sensitive for optical or infrared radiation. It indicates the range of a target continuously and operates fully automatically. It permits detection of a target which is closer than the background and against which it exhibits some contrast and it permits automatic tracking when a relative motion between target and observer takes place. Hence, the system combines an automatic passive optical detector, rangefinder, and homing device. It is thereby insensitive within the limits of signal to noise ratio to the background radiation whatever its intensity might be, and it allows discrimination automatically between many targets within the field of view and in a row of ranges. Since the system employs the method of finding the trigonometric parallax of the target, it is independent of only vaguely determinable quantities (like assumptions about the most probable size or speed of the target) and, therefore, it achieves high accuracy. This accuracy increases in reverse proportion to the distance to the target, hence the system is suited best for short ranges from zero to about 30 miles, if conventional opto-mechanical methods for establishing the base are employed. However, there is no restriction in principle to the length of the base of the measuring triangle, hence much larger distances can be determined by correspondingly large base lengths when the optical signal from the target is of sufficient strength.

Because of the simplicity of its principles, this passive rangefinding system is applicable to many kinds of conventional weapons. Through the addition of more extended automatic evaluation devices, the system can become ideally suitable for guided missiles control and observation. Continuous automatic surveillance of a large space, and detection and observation of targets within this space, and a wide variety of range determinations can be accomplished with equipment using these principles.

II. BASIC PRINCIPLES

This passive rangefinding system measures the parallactic angle of a target (which has to be visible in the optical or infrared spectral region) continuously from the base of a parallactic triangle. It utilizes the fact that a target at finite range is seen from different angles from the two endpoints of the base, and that a background at a much greater distance is seen from essentially the same angle from these endpoints. The angular difference between the lines of sight to the target is used to measure the target distance. The measurement is accomplished by translating position into time. In effect, images of the field of view from the two endpoints of the base are scanned, in phase, and the difference in time required for the target image to reach the same point in the two is used to measure the range. For very great ranges, that is for background far beyond the target, each point in the field of view will be reached at essentially the same time, and there will be no target indicator. If a target much closer to the rangefinding system is present, the time difference measures its distance, while the phase of the scan of which it is encountered determines its direction. To accomplish these ends, the rangefinder forms an optical, or an infrared image of the field of view and translates the brightness values encountered during the scanning into electrical signals, and measures the time difference by electronic means.

III. EXPLANATION OF THE SYSTEM

The mode of operation is illustrated schematically in Figure 1. At the ends, E_1 and E_2 of the base B two image forming objectives, O_1 and O_2, are mounted with their optical axes perpendicular to the base. These objectives form images, I_1 and I_2, in the planes of two slits S_1 and S_2, which are related to two photocells or photomultipliers P_1 and P_2. The two images of a far remote background are essentially identical. Far remote means at a distance that is large compared to the chosen base length. The two images are scanned by the two slits simultaneously, and in phase. Evidently, for the far distant background, for which the light from any given small area comes to the two lenses along practically parallel lines, the outputs of the two photocells will be practically identical (Fig. 2), and if they are connected to oppose one another, will yield zero output. (Fig. 3) If, however, there is a target in the field of view much closer than this background, the photocell outputs will not cancel, since the images I_1 and I_2 of the target will exhibit a different shift relative to the background in the direction of the base (See Fig. 4). The compensated output of the photocells, therefore, will result in net pulses, which start at the left edge of the target image in the left system and last up to the right edge of the target image in the right system (See Fig. 5). If the target image is small compared with its parallactic shift, only narrow pulses will occur and the chain of pulses will be interrupted by background compensated zero output. These narrow pulses could be utilized for range indication, since the distance of their left slopes, for example, is a measurement of the target range (See Fig. 6). If, however, the target image is extended and the parallactic shift is small so that the two images overlap, no range indication can be achieved. To solve this problem, two equal systems as described above in Figure 1 have to be employed. (See Fig. 7.) Every single system will compensate for infinite background and will produce some net signal current as long as a target image is scanned. These net signal currents, however, will exhibit a phase shift to each other, which corresponds to the parallactic angle now seen from the centers of the two systems. (See Fig. 8.) Hence, the centers of the systems form the base of the measuring triangle. (Since such an arrangement permits the automatic range measurement of extended as well as point targets, it is chosen for further explanations.) The moment of scanning time t_1, when in the right system the signal current compensated to zero by infinite background changes into a net signal current because of the uncompensated target image, minus the moment of scanning time t_2, and when the same happens in the left system, is the measurement for the distance of the target. (See Fig. 9.) Since the change from the zero output to a net signal will take place at that part of the extended target image where the contrast against the background is sufficient, both systems will always be triggered by the same or nearly the same part of the image. This is important, to fulfill the necessary condition that the measuring triangle has its apex at the actual target surface. (See Fig. 10.)

The existence of a net pulse, when scanning the field of view, will tell about the existence of an optical target in the field of view, hence this system is an automatic target detection system also. The motion of the net pulse in the field of view will indicate the component of motion of the target in the plane of the scanning direction. If the field of view is divided into two halves with separation perpendicular to the scanning direction, the existence or vanishing of the net signal in one of the halves will indicate the component of motion of the target perpendicular to the target direction. Both components combined make the rangefinder an automatic tracking system.

In practical application, the background does not necessarily have to be in a distance which corresponds to an exact parallelity between the optical axis of the two base endpoints. Even not too small angles of deviation are permitted to keep the two background images equal for compensation; however, these angles must then be known for the range evaluation.

IV. TECHNICAL REALIZATIONS

Several possibilities exist to realize technically the principles described where conventional opto-mechanical elements are employed. Different constructions will be possible whether the scanning is performed at the object or image side, or between object and image side, and whether the two systems necessary for resolving extended targets are separated or not. The arrangement with scanning between object and image side has several advantages because of its simplicity and similarity to conventional rangefinders. (See Fig. 11.)

The base is given by the tube B, the endpoints of which are given by the plane mirrors M_1 and M_2 making angles of 45° with the axis of B. Rays perpendicular to B and under 45° to M_1 and M_2 coming from the object side will be reflected into the direction of the axis. A rotatable double faced plane mirror $M_{3,4}$, with its axis of rotation A perpendicular to B and to the incoming perpendicular rays, is located in the endpoint of B. Between M_1 and $M_{3,4}$ are the objective lenses O_1 and O_2 with their focal planes F_1 and F_2. F_1 and F_2 are located parallel to the axis B and to the axis A of rotation when mirror $M_{3,4}$ has a position 45° to the direction B. In these focal planes are the slits S_1 and S_2 parallel to A and opposite to B. Behind the slits are the photodetectors P_1 and P_2 (photomultipliers) which feed signals into the electronic circuitry C. The infinite (far remote) background ∞ will form images I_1 and I_2 in F_1 and F_2. When $M_{3,4}$ rotates, the images will move over the slits S_1 and S_2, exchange place with S_2 and S_1 and repeat a scanning twice every rotation. The integrated light flux from the image details, which move over the slit area (x·y) during rotation of $M_{3,4}$ passes through the slit and illuminates the photocathode of the photomultiplier P_1 or P_2 respectively. If the background exhibits image details at all, the same details will move at the same time over slit S_1 and slit S_2, and the same photocurrents will therefore be produced by P_1 and P_2. These photocurrents are combined after proper amplification, in the electronic mixer stage for instance, or double grid tube, with opposite polarity. Their opposite effects on the grids will cancel any effect on the anode current and no signal current will result in the output of C. If, however, the image details falling upon slits S_1 and S_2 are different, then a signal will occur in the output of C. The amplitude and the slope angle of this signal will be used to trigger, in a multivibrator circuit, a rectangular pulse which lasts for the time of scanning one image. This is done by switching off the multivibrator by a secondary time signal when the edge of the image passes the slit.

Since two equal systems of the described kind are employed and both systems form the base of the measurement triangle, two rectangular pulses result, one for each system. (See Fig. 12.) These two pulses now have a time shift which corresponds to the parallactic angle of that detail in the optical object which caused an uncompensated net signal in each system. Hence, both rectangular pulses mixed electronically in a third mixer stage with opposite polarity result in a differential pulse, the duration of which measures the distance, and the time phase of which against the secondary time signal measures the speed component in the scanning direction of that image detail which cannot be compensated. Such detail, of course, belongs to the target because the target is closer than the background. Since the distance measurement depends on the instants the two rectangular pulses are triggered, the rotational speed of the rotating double faced mirrors in the two systems must be equal, or possible deviations from equality must be accurately known.

With the rotating mirror $M_{3,4}$ another rotating or oscillating stop is mechanically coupled which covers the upper or lower halves of the slits S_1 and S_2 every second image, which is scanned without the stop in the field of view. Hence, when no stop is in the field of view the circuit will detect a target in the moment a net signal occurs, and it will measure range and tangential speed of this target. Then with the next image where, for instance, the upper half of it is covered by the stop the circuit will check whether the net signal is still there. If the net signal does not occur, the rangefinder systems will be corrected in the direction perpendicular to the base so much until the net signal vanishes in the lower half, and so forth.

The repetition rate of images to a dead time interval where no scanning takes place is unfavorable in case of the rotating plane mirror. It can be considerably increased when a rotating drum with slits on its peripherie is employed. The photodetectors have to be inside the drum or optical elements have to change the light path. It is likewise possible to move the images across the slits by synchronized motion of mirrors at the object side in front of the base ends. This system permits scanning of large angles of view. Finally, instead of moving the images across the slits, the slits can by synchronously moved across the firm images for instance by an oscillatory motion. In this case an arrangement where the optical axes are perpendicular to the base might be of advantage, since sensitive optical systems of high aperture ratio can be employed, which can constitute a very large base length. Deviations from synchronism of the oscillating slit mechanism can be measured optically or electronically and can correct the range measurements.

Electron optical means instead of opto-mechanical means are likewise applicable for realizing the principles of the passive rangefinding system. When, instead of the relative motion between image and slits, the scanning of the images by electron beams is introduced the mechanical system can be converted into an electronic system. Orthicons are arranged at the base ends and the electron beams are synchronized. The target plates of the orthicons have equal charge distribution, when only the infinite background is imaged on the photocathodes of the orthicons. The image pulses are equal when the target plates are scanned synchronously. They can, therefore, be compensated. If an optical object is in parallactic range, it will be differently located at the target plates, hence scanned at different times, and a net pulse will result. All the other operations of the system can be solved analogously to the opto-mechanical system.

V. CALCULATIONS

THE RANGE

Since the automatic passive rangefinder system is based on a triangulation, the following relations for the range R are valid. (See Fig. 13.)

$$R = \frac{B \cos\beta}{\sin(\alpha - \beta)}$$

and for $\beta = 0$

$$R = \frac{B}{\sin\alpha}$$

The parallactic angle η usually is very small, hence with sufficient accuracy

$$\eta = \frac{B}{R}$$

If an error $d\eta$ is made in measuring this angle, the corresponding error dR in range is given by

$$dR = -\frac{R^2}{B}\, d\eta$$

When the target is not a well defined point or line normal to the plane of measurement, the error in range is given by

$$R' - R = B\left(\frac{1}{\sin\alpha'} - \frac{1}{\sin\alpha}\right)$$

and

$$C = \frac{R \sin(\alpha - \alpha')}{\cos\alpha'} = \frac{B \sin(\alpha - \alpha')}{\sin\alpha \cos\alpha'}$$ (See Fig. 14.)

THE CONTRAST SENSITIVITY

It is of interest to derive for the system, an expression which contains the main parameters influencing the automatic measurement. Such an expression would then hold, when properly applied, for the various possible modifications of the system which were indicated above. Chiefly the following parameters have to be considered.

E_1		Brightness of the target (candles/cm^2)
E_o		Brightness of the background (candles/cm^2)
E	$E_o - E_1$	contrast background to target (candles/cm^2)
x		Width of scanning slit (cm)
y		Length of scanning slit (cm)
D		Diameter of objective lens (cm)
f		Focal length of objective lens (cm)
A	$\frac{D}{f}$	aperture ratio
α	$\frac{x}{f}$	angular width of slit (degrees)
β	$\frac{y}{f}$	angular length of slit (degrees)
n	$\frac{\omega}{2\pi}$	rotational speed of scanning mirror (rps)
d	ϕf	distance between mirror axis and slit
ν_ζ	$4n$	frequency of measurements
τ		Time needed for an image point to traverse the slit
ν_μ		Upper frequency limit of the photoelectric circuit
S_c		Sensitivity of the photodetector
V_s		Signal voltage
V_n		Noise voltage

s $\frac{V_s}{V_n}$ signal to noise ratio

V Velocity

T Absolute temperature

b Parallactic angle

K Boltzman constant

I Photoelectric signal current

S_r $\frac{1}{E_{min}}$ contrast sensitivity of rangefinder

In one proposed arrangement of the opto-mechanical rangefinder, the image of the target in range R is formed by an objective with aperture ratio A on the slit plane after it was reflected from a rotating mirror. The distance between mirror axis and slit (x y) is d. The target area focused on the slit area is $\frac{xy}{f^2} R^2$

The light flux from this target area, which passes the objective is

$$\Phi_1 = E_1 \frac{xy}{f^2} \frac{R^2}{R^2} \frac{\pi D^2}{4} = E_1 \frac{xy}{f^2} \frac{\pi D^2}{4} \text{ lumen}$$

and, introducing angular quantities this becomes

$$\Phi_1 = E_1 \frac{\alpha \beta \pi D^2}{4} .$$

A corresponding relationship is valid for the light flux from the background $\Phi_0 = E_0 \frac{\alpha \beta \pi D^2}{4}$

Assuming that the edge of the target image is a straight line parallel to the slit and extends over the whole length of the slit, the change in the light flux Φ passing the slit when the image is swept by the rotating mirror is $\Delta \Phi = E \frac{\alpha \beta \pi D^2}{4}$

where E is the contrast difference in the radiation intensity between target and background. Corresponding to this change of light flux a change in the photocurrent of the cell arises. If the sensitivity of the cell is S_c, the signal current produced by the contrast E becomes

$$I = S_c E \frac{\alpha \beta \pi D^2}{4}$$

The next step is the determination of the minimum photocurrent change, which can be detected by a conventional amplifier. Let us consider a most simple circuit. The signal voltage V_s produced by the current change I is obviously $V = I r_L$ where r_L is the load resistor. Assuming as usually a minimum permissible signal to noise ratio $s = \frac{V_s}{V_n} = 1$, we must choose a load resistor r_L corresponding to a noise voltage $V_n = V_s$. Since noise voltage and resistor are related by the well known formula

$$V_n = \sqrt{4 kT r_L \Delta \nu}$$

where k is the Boltzman constant and T the absolute temperature, we obtain

$$I^2 r_L^2 = 4 kT r_L \Delta \nu$$

or

$$r_L = \frac{4 kT \Delta \nu}{I^2}$$

The lower limiting frequency of the amplifier may be neglected in comparison with the upper limiting frequency ν_u, $(\nu_u \ll \Delta \nu)$. ν_u is determined by

$$r_L = \frac{1}{2 \pi \nu_u (C_i + C_c)}$$

with C_i input capacitance of amplifier, C_c capacitance of photocell, and we get

$$\frac{1}{2 \pi \nu_u (C_i + C_c)} = \frac{4 kT \Delta \nu}{I^2}$$

or

$$I = \sqrt{8 \pi kT (C_i + C_c) \nu_u}$$

This is the minimum signal current which can be separated from the noise. It corresponds to the minimum detectable contrast

$$E_{min.} = \frac{4\,\nu_u\sqrt{8\pi kT\ \ C_i + C_c}}{S_c\,\alpha\,\beta\,\pi\,D^2}$$

The formula shows that the indication of contrasts is the more sensitive the lower the upper frequency limit is chosen. Since this frequency limit is determined by the frequency ν_s of the scanning device, ν_u should be replaced by ν_s, where ν_s is found by application of the following relations being valid for the rangefinder:

If n is the rotational frequency of the scanning mirror, the scanning frequency ν_s is 4n sec^{-1}. The distance between the rotation axis of the mirror and the slit was $d = \psi f$. Hence, the image is swept over the slit with the velocity, v

$$v = 2\omega d = 4\pi n d = \pi \nu_s d = \pi \nu_s \psi f$$

Therefore, the time during which an image spot passes the slit of the width x is

$$\tau = \frac{x}{v} = \frac{\alpha}{\pi\,\psi\,\nu_s}$$

The upper frequency limit is reverse proportional to the value of time, therefore

$$\nu_u = \frac{1}{\tau} = \frac{\pi\,\psi\,\nu_s}{\alpha}$$

$$E_{min.} = \frac{4\sqrt{8\pi kT\ (C_i + C_c)}\ \psi\,\nu_s}{S_c\,\alpha^2\beta\,D^2}$$

This formula shows that the minimum discernable contrast decreases rapidly with increasing angular width of the slit. Likewise, the relative error p of the measurement is reduced by increasing the slit width. Basically, the function of the rangefinder is to measure the angles γ, where $\gamma_1 + \gamma_2$ is equal to the parallactic angle η. The target may be supposed to be seen in a direction perpendicular to the base line B. Because the angle η is determined by sweeping the image of the target over a slit with an angular width α, the uncertainty of this determination cannot be greater than α. Since $R = \frac{B \operatorname{tg} \eta}{2}$

and $\frac{dR}{d\eta} = \frac{B}{2} \frac{1}{\cos^2\eta} = \frac{B}{2}(1+\tan^2\eta)$, we obtain $dR = \frac{B}{2}(1+\frac{4R^2}{B^2})\, d\eta$

Because $(\frac{R}{B})^2 \gg 1$, dR is about equal to $\frac{2R^2}{B} d\eta$ and the relative error p of the distance measurement becomes

$$p = \frac{dR}{R} = \frac{2R}{B} d\eta = \frac{2R}{B} \alpha$$

This relation can be used to introduce the relative error instead of the slit width into the formula for the minimum contrast. The inverse value of the minimum contrast may be called the contrast sensitivity S_K of the rangefinder in general. It is given by the proportion

$$S = \frac{1}{E_{min}} \propto \frac{S_c\, B^2\, p^2\, \beta\, D^2}{8\, R^2\, \psi \nu_5 \sqrt{8\pi\kappa\, T(C_c + C_c)}}$$

where $k = 1.374 \times 10^{-23} \frac{\text{watt sec}}{\text{degree Kelvin}}$

$T = 293$ degree Kelvin

$C_i + C_o = 8 \times 10^{-12}$ Farad

NOISE CALCULATION FOR PHOTOMULTIPLIERS

If the background portion of the beam which is focused onto the slit has the area $\frac{xy\ R^2}{f^2}$ and its brightness is E_o candles/cm^2, then the luminosity of this portion of the slit is $\frac{xy\ R^2}{f^2} E_o$. Hence, the light flux from this background area falling on the lens with diameter D would be

$$\Phi_o = \frac{xy\ R^2}{f^2} E_o \frac{\pi D^2}{R^2}$$

The background light flux per unit length of the slit becomes

$$\Phi_o = \frac{x E_o \pi D^2}{4 f^2} T \text{ lumen/cm}^2$$

where T is the optical transmission factor. If E_1 is the brightness of the target, the target light flux per unit length of slit correspondingly becomes

$$\Phi_1 = \frac{x E_1 \pi D^2}{4 f^2} T \text{ lumen/cm}^2$$

We assume now that the target has a higher brightness than the background, $E_1 > E_o$. If the target with a true height H is inside the slit area, it covers a background area with a height H_1 and for the whole slit area the light flux increases since E_1 is greater than E_o, by the value $\Phi_o - \Phi_o(H) + \Phi_1(H)$ or, since the image of the target being in a distance R has the dimension $\frac{Hf}{R}$, we get for the abrupt increase of light flux when the target comes into the slit,

$$\Phi_o - (\Phi_o - \Phi_o(H) + \Phi_1(H)) \quad \text{or} \quad \Phi = \frac{H}{R} \frac{x}{f} \frac{\pi D^2 T}{4} (E_1 - E_o) \text{lumen}$$

A multiplier with a cathode sensitivity S_c and a current amplification factor C together with a load resistor R_L, transforms this abrupt increase in illumination to a signal voltage of

$$V_s = \frac{H}{R} \frac{x}{f} \frac{\pi D^2 T}{4} (E_1 - E_0) S_c C R_L \text{ volts}$$

or
$$V_s = \frac{Hf}{R} (\Phi_1 - \Phi_0) S_c C R_L$$

This equation • gives the change in the light flux; i.e., the change from background signal to background plus signal. We now calculate the total noise first for the combined illumination by target and background. We can write the total light flux passing the slit for this case in the form $\Phi_t = \Phi_1 \frac{Hf}{R} + \Phi_0 \left(y - \frac{Hf}{R}\right)$

or
$$\Phi_t = \frac{Hf}{R} (\Phi_1 + \Phi_0) + \Phi_0 y$$

This illumination results in a primary photocurrent given by

$$I_p = \Phi_t S_c = S_c \left(\frac{Hf}{R}(\Phi_1 + \Phi_0) + \Phi_0 y\right)$$

This current together with the dark current I_α contains a noise component given by $I_{np} = \sqrt{2e\left[S_c\left(\frac{Hf}{R}(\Phi_1 - \Phi_0) + \Phi y\right) + I_\alpha\right]\Delta\nu}$

e means electron charge

Now we can replace the dark current I_α by a light flux per length unit of the slit Φ_α, which produces a photocurrent equal to I_α i.e.,

$\Phi_\alpha = \frac{I_\alpha}{S_c y}$ If we put this expression into the foregoing equation we get

$$I_{np} = \sqrt{2e \; S_c\left[\frac{Hf}{R}(\Phi_1 - \Phi_0) + y\,(\Phi_0 + \Phi_\alpha)\right]\Delta\nu}$$

The parenthesis of this equation contains two components of the light flux. The first part: $\frac{Hf}{R}(\Phi_1 - \Phi_0)$ means the increasing of illumination by the target. The second part: $y(\Phi_0 + \Phi_\alpha)$ means a constant. Now we may introduce a factor δ representing the relative changing of the light flux caused by interference from the target

$$\rho = \frac{Hf}{Ry} \quad \frac{\Phi_1 - \Phi_0}{\Phi_0 + \Phi_\alpha}$$

Setting this expression into equation above we get

$$I_{np} = \sqrt{2 e S_c \left[\frac{Hf}{R}(\Phi_1 - \Phi_0)\left(1 + \frac{1}{\rho}\right)\right] \Delta \nu}$$

and the voltage of the noise due to the output becomes

$$V_n = FCR_L \sqrt{2 e S_c \left[\frac{Hf}{R}(\Phi_1 - \Phi_0)\left(1 + \frac{1}{\rho}\right)\right] \Delta \nu}$$

Here F is the contribution to the noise by secondary electrons emitted by the dynodes of the photomultiplier. Comparing this formula with the signal voltage, the signal to noise ratio becomes

$$s = \frac{V_s}{V_n} = \frac{1}{F} \frac{\sqrt{\frac{Hf}{R}(\Phi_1 - \Phi_0) S_c}}{\sqrt{2e\left(1 + \frac{1}{\rho}\right)\Delta \nu}}$$

Since $\Phi_1 - \Phi_0 = (\Phi_0 + \Phi_\alpha)\, \rho \frac{Ry}{Hf}$, we got

$$s = \frac{1}{F}\sqrt{\frac{S_c}{2e\Delta\nu}(\Phi_1 + \Phi_\alpha) y \frac{\rho^2}{1+\rho}}$$

For δ>>1, i.e., for an extended target image, great contrast, and weak background illumination, this expression becomes

$$s = \frac{1}{F}\sqrt{\frac{S_c}{2e\Delta\nu}(\Phi_0 + \Phi_\alpha) y \rho}$$

or

$$s = \frac{1}{F}\sqrt{\frac{S_c}{2e\Delta\nu} (\Phi_1 - \Phi_0)\frac{Hf}{R}}$$

For $\delta >> 1$, i.e., for a small target image, small contract, and strong background illumination, this expression becomes

$$s = \frac{\rho}{F}\sqrt{\frac{S_c}{2e\Delta\nu}(\Phi_0 + \Phi_\alpha)}$$

or
$$s = \frac{1}{F}\sqrt{\frac{S_c}{2e\Delta\nu}}\;\frac{\Phi_1 - \Phi_0}{\sqrt{\Phi_0 + \Phi_\alpha}}\;\frac{Hf}{R\sqrt{y}}$$

In the foregoing section expressions for noise caused by a combined background-target illumination were developed. Now we develop the expression for noise caused by background only. The total light flux passing the slit in this case can be written in the form $\Phi_t = \Phi_0 y$

This illumination results in a primary photocurrent $I_p = \Phi_t S_c = \Phi_0 y S_c$

This primary photocurrent together with dark current I_α causes a noise current $I_{np} = \sqrt{2e(\Phi_0 y S_c + I_\alpha)\Delta\nu}$

Again introducing $\Phi_\alpha = \frac{I_\alpha}{S_c y}$, we get $I_{np} = \sqrt{2eyS_c(\Phi_0 + \Phi_\alpha)\Delta\nu}$

and with
$$\rho = \frac{Hf}{Ry}\;\frac{\Phi_1 - \Phi_0}{\Phi_0 + \Phi_\alpha}$$

this equation becomes $I_{np} = \sqrt{2eyS_c\frac{Hf}{Ry}(\Phi_1 - \Phi_0)\frac{1}{\rho}\Delta\nu}$

and
$$V_n = FCR_L\sqrt{2eS_c\frac{Hf}{R}(\Phi_1 - \Phi_0)\frac{1}{\rho}\Delta\nu}$$

Comparing this formula with the signal voltage, the signal to noise ratio becomes

$$s = \frac{V_s}{V_n} = \frac{\frac{Hf}{R}(\Phi_1 - \Phi_0)S_c C R_L}{FCR_L\sqrt{2eS_c\frac{Hf}{R}(\Phi_1 - \Phi_0)\frac{1}{\rho}\Delta\nu}}$$

or
$$s = \frac{1}{F}\sqrt{\frac{S_c}{2e\Delta\nu}(\Phi_1 - \Phi_0)\frac{Hf}{R}}$$

or
$$s = \frac{1}{F}\sqrt{\frac{S_c}{2e\Delta\nu}}\,\frac{(\Phi_1 - \Phi_0)}{\sqrt{\Phi_0 + \Phi_\alpha}}\,\frac{Hf}{R\sqrt{y}}$$

and that is the same equation as the equation for $\delta \ll 1$.

Substituting $\Phi_0 = \frac{x E_0 \pi D^2}{4 f^2} T$ again into the main noise formula, we obtain

$$s = \frac{1}{F}\sqrt{\frac{S_c}{2e\Delta\nu}}\sqrt{\left(\frac{x\pi D^2 T}{4f^2}E_0 + \frac{I_\alpha}{S_c y}\right)y}\;\frac{\rho^2}{1+\rho}$$

This equation now allows the calculation of the maximum bandwidth, for instance for a signal to noise ratio s=1.

$$\Delta\nu = \frac{1}{F^2}\,\frac{1}{2e}\left(\frac{\pi}{4}\,\frac{D^2}{f^2}\,xy\,E_0 S_c T + I_\alpha\right)\frac{\rho^2}{1+\rho}$$

According to the last equation, we are able to accomplish a numerical evaluation for the maximum scanning frequency depending on the bandwidth $\Delta\nu$.

Let

e	$= 1{,}6\cdot 10^{-19}$ coul	T	$= 0{,}7$
F	$= 2$	$\left(\frac{D}{f}\right)^2$	$= 4\cdot 10^{-2}$
x	$= 4\cdot 10^{-3}$ cm	S_c	$= 30.10^{-6}$ A/lum
y	$= 2{,}5$ cm	I_α	$= 10^{-14}$A

Thus we get
$$\Delta\nu = \frac{10^{19}}{4\times 3.2}\left(\frac{\pi}{4}\,10^{-2}\times 4\times 10^{-2}\times 0.7\times 30\times 10^{-6}\times E_0 + 10^{-14}\right)\times\frac{\rho^2}{1+\rho}$$

Hence we obtain $\Delta\nu$ as a function of ρ with the parameter E_0 in the form:
$$\Delta\nu = 7.8 \times 10^{17}\,(66 \times 10^{-10}\,E_0 + 10^{-14})\frac{\rho^2}{1+\rho}$$

Table I shows the dependency of the maximum frequency bandwidth on the ratio $\rho = \frac{Hf}{Ry}\,\frac{(\Phi_1 - \Phi_0)}{(\Phi_0 + \Phi_\alpha)}$ and the parameter E_0 (brightness of the background measured in Stilb from 0.5 down to 0.0001 Stilb, where 1 Stilb = 1 candle/cm^2).

VI. DESIGN OF WORKING MODEL AND EXPERIMENTATION

GENERAL MECHANICAL DESIGN AND DIMENSIONS OF A WORKING MODEL

To prove the principles and calculations given above, a working model was designed and built. It is shown in Figure 15. Spatial limitations and the difficulty of synchronizing the two rotating scanning mirrors of the complete four beam range finder system electro-mechanically brought about a variation of the system, where only three beams are employed. Such a construction permits the combination of the two medium "eyes" into one and has both scanning mirrors rotating on the same shaft by which synchronization is guaranteed. This design, however, has many related constructive inconveniences and a much lower rate of performance is respect to sensitivity and speed of control, since one period of pulses is always lost and the optical systems do not match because of necessary differences in design.

To perform measurements about the sensitivity and signal to noise ratio of photomultipliers when illuminated by a background target area through a slit, and to compare two systems parallactically directed to the same target, another instrument was designed and built. It is shown in Figure 16. Two Zeiss photographic objectives f:5 of 50cm focal length illuminate, through adjustable slits of 1cm length, the interior of a light integrating mirror box each. Each box contains an adjustable photomultiplier (RCA IP21) and a cylindrical lens to distribute the light from the slit image over the photocathode.

The realization of the three-eyed optical range finder incorporating the double binocular systems, described above, raised certain problems. While the difficulty of synchronizing all (passive) scanning beams was principally overcome by using a common revolving system, it became necessary to have the center eye work in an elevated plane, since one of the revolving mirrors had to be placed higher than the other. Furthermore, a wrong course of pulses had to be cancelled out. These wrong pulses develop when the revolving mirrors get into the 135° and 315° positions when the oncoming pictures are projected into the wrong photocells; while the 45° and 225° positions, as shown in the figures, are accepted to produce the right effects. The design provides a choice between two different methods for cancelling out the unwanted pulses: (1) by means of mechanically revolving shutters (similar to those used in movie projectors) or (2) by means of generating control pulses by magnetic induction, so that an electronic blanking can be achieved. The electronic method has been used in the working model discussed here. The essential details of the mechanical design, and the main dimensions are shown in Figure 17, while Figure 18 shows all parts disassembled.

As already mentioned, the optical system works on two slightly displaced levels, eye Nr. II being 2-3/4 inches elevated above the other one for eyes Nrs. I and III. This, however, should not matter at all when the relatively much larger ranges (from 300 ft. to 6000 ft.) are to be covered by the instrument. There are two additional levels (along the common shaft) required for proper operation. One level is located a little above the mirror for eye Nr. II; its concern is to provide the driving mechanism, while the control pulse generating device is incorporated somewhat underneath the lower mirror for eyes Nrs. I and III.

In the space between both mirrors, the drive gear for the revolving shutters is provided as a precautionary additional means for blanking out the wrong pulses referred to above.

The focal length of each lens system quite obviously is made equal (19.5 inches), so are the slit widths (1/10 mm). The condensing cylinder lenses are fairly equal, and the multipliers (photocells) were selected from a number of cells to find those most similar. The pulse generator delivers pulses whose opening and closing blanks are 8-1/2° apart, in accordance with the usable field of view. Eye Nr. II had to be placed in the center of the apparatus causing an eccentricity of 3-3/4 inches of the revolving system. All lenses have different distances from their particular end mirrors which are shown in brackets in Figure 17.

As was shown in Figure 13, the range D to the target T can be calculated with sufficient accuracy by means of the relation: $\gamma D=B$, or $D=\frac{B}{\gamma}$, where B is the Base of the Range Finder=40 inches. γ can as well be expressed by the direction $\Delta\alpha_{\tau} = \alpha_{\tau} - \alpha_{I\tau}$ of the scanning beams, which is directly dependent on the momentary angular position of the revolving system, and therefore can be expressed by the angle ϕ_{τ}. Angle ϕ_{τ} however, is to be indicated by the integrating measuring device as fraction of a half turn or repetition time (of RM), that means the indicator shows $\frac{\phi_{T}}{180}$. Now, what is the relation between and ϕ? Here the actual dimensioning of the range finder has to be taken into consideration. Angular relations can be derived as seen in Figure 19. $90 - (45° - \phi + \beta) = 45° - \phi + \alpha : \phi = \frac{\alpha+\beta}{2}$

for small angles (ϕ 45°): $a \times \alpha = b \times \beta$

$$17 \times \alpha = 2.5 \times \beta \quad \frac{\beta}{\alpha} = 6.8$$

In eliminating β we find: $\phi = 3.9$. Let's suppose a linearity between ϕ and α all around a circle. A full sequence (repetition) means ϕ = 180° as a result the maximum imaginable field of view would be $\alpha_{180°}$ = 46°. The size of the actual field of view naturally can only be a fraction thereof because of certain limitations. There is an obstruction of the full viewing channel by the tubular case, particularly in the longer right leg and also by the limited length of the revolving mirrors. But, the main limitation is the nonlinearity between ϕ and α which must be kept low within the field range. Careful calculations showed that the variations of the nonlinearity resembles a parabolic curve with zero in the central viewing point and going as high as 1/5 of 1% in the edges of the size of the field of view which is considered acceptable. Since the scanning beams always wander across identical areas of the revolving mirrors, exact compensation is therefore maintained. But the nonlinearity affects the indication of the range up to 1/5 of 1% depending on the area within the field of view where the target is located. Further calculations showed that these conditions are practically the same in the working model in which revolving mirrors of a material thickness of 1/8 inch are used. It influences essentially the mean position of the revolving mirrors, which decrease from 45° to a little less than 44° 30', the highest and lowest useful angles of the revolving mirrors are 48° 55' and 40° 25' respectively, hence compassing an angle ϕ = 8° 30'.

Data

Base length of range finder	B = 40 inches
Repetition after 1/2 turn of revolving mirrors or	180°

Exploitable angular movement of revolving mirrors	$\phi = 8° 30'$
or in fraction of repetition 8.5/180 = 1/21 or	4.7%
Field of view (with $\phi = 3.9\alpha$, $\phi = 8° 30'$)	$\alpha = 2° 10'$
Speed of revolution of revolving mirrors = 390 RPM	6.5 RPS
Repetition rate (mirrors silvered on both surfaces)	13 frames per sec
Time for one repetition period	77 MS
Duration of one scanning (frame) 4.7% x 77 MS	= 3.6 MS
Angular speed of scanning $\frac{d\alpha}{dt} = \frac{2° 10'}{16}$	.60 ρ/ms
Linear speed of scanning in focal plane (slit)	5.2 mm/ms
Nonlinearity of scanning speed	$\leq$ .2%
Focal length of main lens systems (495 m/m)	19.5 inch
Slit width	.1 m/m
Angle formed by slit width and focal length $\frac{.1}{495} \times 57.3$	.0116°
Time for Scanning of Slit Width = Rise Time of Pulse	$\frac{.0116}{60} = 19.5\ \mu s$
Size of field of view (in focal plane-slit 1) height	19 m/m = .75 inch

CLOSEST RANGE TO A MEASURABLE TARGET

It has to be realized that the target must be seen clearly within the fields of view of all three eyes, possibly within about 60% of the field width. A triangulation results in:

$$D_{min} = \frac{B}{\alpha\ 60\%} = \frac{2B}{\alpha\ 60\%} = \frac{2 \times 80}{1.3} \times \frac{57.3}{12}$$

$$D_{min} = 300 \text{ ft.}$$

The range in general would be: $D = \frac{B}{\psi} = \frac{B}{\Delta \alpha_t}$

with $\alpha = \frac{d\alpha}{dt} \times t$.

Therefore $D = \frac{B}{\frac{d\alpha}{dt}} [in] \frac{57.3}{12}$ ft.

Since the repetition time is T = 77 ms, and since the apparatus is supposed to give an indication proportional to the quotient $\frac{t}{\tau}$ $(t = \frac{t}{\tau}\ 77)$, D becomes $\frac{40}{60} \times \frac{57.3}{12} \times \frac{1}{t} = \frac{320}{t[ms]}$ [ft].

We may also write the above equation for the value of D as follows:

$$D = \frac{320}{77 x \frac{t}{\tau}} = \frac{4.2}{(t_\tau)} \text{ ft.}$$

The maximum range which can be covered by the sample device depends widely on what amount of misinformation is acceptable, and what accuracy of alignment can be achieved and maintained during the operation. Assume that all errors can be expressed in terms of misalignment of the slit which supposedly may be kept down to 1/2500 inch (1/100 mm). This represents an angle $\Delta\alpha$ = .00116° and a corresponding scanning time of t = 1.95 s. Hence, the range indication would be $D_f = \frac{320}{t \pm \Delta_\tau}$ or the inaccuracy over the range:

$$\Delta D_f = \frac{D - D_f}{D} \times 100\% = (1 - \frac{t}{t \pm \Delta t}) \times 100 \ \frac{\pm \Delta t}{t \pm \Delta t} \times 100 = \frac{\pm 95}{\frac{320,000}{D}} \pm 1.95\%$$

Until now it has been taken for granted that the pulses induced by an arbitrary target were sufficiently strong for the operation of the range indicating device. It is quite obvious that the strength (amplitude) of the pulses depends partly on the mean luminosity in the slit while crossing (touching) the target in comparison to that of a previous time element, and partly on the brightness of the scanned area itself. A fairly even radiating sky and relatively dark target of a rectangular shape are presumed in the following example: (See Fig. 20.) $\delta = \frac{h}{H} = \frac{h_T}{.75 in}$ [ft] $\times \frac{19.5 in}{D\ ft} = 26 \frac{h_T\ ft}{D\ ft}$

Where h_T = Height of Target

D = Range

H = Length of slit

h = Height of image of target

Contrast = Log $\frac{J_1}{J_2}$ definition

Mean Brightness in Slit Area:

(1) including target: $J_1\ (1-\alpha) + J_2\alpha = J_m$

(2) area without target: J_1

Change of resulting photo current $P = \frac{J_1 - J_m}{J_1} \times 100$ in per cent of J_1 current or $P = \alpha\ (1-\frac{J_2}{J_1}) \times 100\%$.

The reverse value is: $\frac{J_m}{J_1} = 1 - \frac{P}{100}$

These equations are useful in determining and evaluating the lower limits of the working conditions of the range finder. That means a value P_{min} can be found which is an apparatus constant for the lowest working limit or threshold. Since $\frac{J_1}{J_2}$ can be found by separate contrast measurement, the contrast must be known in this case. Furthermore, it is significant to know that it has proven suitable to keep the photo current caused by $P \times J_1$ at almost a constant level regardless of the absolute brightness. This is profitable as far as the electronic circuits then work with nearly constant input voltage, which makes for better stability. According to this manner of control, the influence of the brightness is widely suppressed onto a point where in very low brightness the noise level becomes relatively evident and causes a failure of the range indication.

VII. EXPERIENCES WITH THE WORKING MODEL

Numerous tests showed the capabilities as well as the limitations of the working model. The latter ones have been referred to before concerning the lowest possible visible contrast and the lowest brightness to work with.

Though the knowledge of the lowest contrast to work with is of some theoretical value in determining the possibilities of the apparatus, it says little about its application against an actual target, e.g., an airplane. While the contrast of a fixed target stays constant for quite a time, it changes considerably, sometimes within split seconds when an airplane is being tracked. In bright sunshine the contrast may even change its polarity; or it may become zero temporarily. Nevertheless, it seemed justified for experimental purposes to replace an actual target, assuming average illumination and a mean contrast, by a fixed target.

Since such a target should not disturb the range indication by the fact that usually some part of the foreground is in the field of view, targets had to be mounted high in the air and at a large distance. The area on top of a hangar between a tower and the roof was considered a suitable place. Two flat metal plates 2 x 2 ft. were arranged there in a distance of 1340 ft. Figure 21 shows these targets.

Now the question arises, how does this target plate behave and what do the pulses look like. The width of the target plate is 2 ft. It is subtended by an angle $\alpha_T = \frac{2}{1340}\,57.3 = .086$, if D = 1340 ft. is the range. With $\frac{d\alpha}{dt} = .60$ o/ms time for scanning the target t_T becomes .086/.60 ms = 144 μs or about seven times as long as the scanning of the slit width.

Hence, the shape of a single pulse is trapeze-like, and consists of three parts:

rise time, (scanning time of the slit width) and decline time the total duration of the pulse (pulse width) is $t_p = 19.5 \mu s$ while the repetition time is T = 77 ms and the time quotient which indicates the range is $\frac{t}{T} = \frac{.240}{77} = .00312$ the range therefore becomes $D = \frac{42}{t/T} + \frac{4.2}{.00312} = 1340$ ft.

Unfortunately the actual pulses do not show up on the scope as trapeze-like as sketched above but rather as triangular, possibly due to smoothing effects of different R-C combinations. As a means of stabilizing the unavoidable pulse jitter it was thought that the best method would be to simulate the characteristics of a thermo-couple instrument, mostly because of its non-oscillating properties. The measuring pulses are, therefore, transformed into minute amounts of electric charge ($\int dt$); they accumulate in a capacitor whose rate of discharge is so dimensioned that when a state of equilibrium is reached the mean charge of the capacitor represents the reciprocal of the range.

There was another trouble spot in the present range finder. It is the centrally located eye jointly used by both comparator systems. The performance could be greatly improved by a complete separation, at least electronically, into two comparators.

After several minor changes in the design of the three eyed range finder model and the electronic circuitry, the end results of many tests became:

Maximum Range		6000 ft.
possible error 50 ft.	at 2000 ft.	

Minimum Range	300 ft.
Lowest mean brightness of scanned area	50 footlamberts
Lowest Contrast	$\log \left(\frac{I1}{I2}\right)_{min} = 0.00045$

(i.e., the target must cover at least 0.108% of slit area with high contrast >3 against sky).

TABLE I

Maximum Frequency Bandwidth as
a Function of Image Brightness
and the Parameter ρ

ρ	$\frac{\rho^2}{1+\rho}$	E_o 0.5 $\Delta\nu$	0.2 $\Delta\nu$	0.1 $\Delta\nu$	0.05 $\Delta\nu$	0.01 $\Delta\nu$	0.001 $\Delta\nu$	0.0001 $\Delta\nu$
0.01	0.0001	$2.57\cdot10^5$	$1.03\cdot10^5$	$5.15\cdot10^4$	$2.57\cdot10^4$	$5.15\cdot10^3$	$5.15\cdot10^2$	$5.3\cdot10$
0.05	0.0024	$6.17\cdot10^6$	$2.47\cdot10^6$	$1.24\cdot10^6$	$6.17\cdot10^5$	$1.24\cdot10^5$	$1.24\cdot10^4$	$1.27\cdot10^3$
0.10	0.009	$2.31\cdot10^7$	$9.27\cdot10^6$	$4.63\cdot10^6$	$2.31\cdot10^6$	$4.63\cdot10^5$	$4.63\cdot10^4$	$7.77.10^3$
0.30	0.069	$1.77\cdot10^8$	$7.11\cdot10^7$	$3.55\cdot10^7$	$1.77\cdot10^7$	$3.55\cdot10^6$	$3.55\cdot10^5$	$3.66\cdot10^4$
0.50	0.17	$4.37\cdot10^8$	$1.75\cdot10^8$	$8.75\cdot10^7$	$4.37\cdot10^7$	$8.75\cdot10^6$	$8.75\cdot10^5$	$9.01\cdot10^4$
1.00	0.50	$1.29\cdot10^9$	$5.15\cdot10^8$	$2.57\cdot10^8$	$1.29\cdot10^8$	$2.57\cdot10^7$	$2.57\cdot10^6$	$2.65\cdot10^5$
2.00	1.33	$3.42\cdot10^9$	$1.37\cdot10^9$	$6.85\cdot10^8$	$3.42\cdot10^8$	$6.85\cdot10^7$	$6.85\cdot10^6$	$7.05\cdot10^5$
5.00	4.17	$1.07\cdot10^{10}$	$4.30\cdot10^9$	$2.15\cdot10^9$	$1.07\cdot10^9$	$2.15\cdot10^8$	$2.15\cdot10^7$	$2.21\cdot10^6$
10.00	9.09	$2.34\cdot10^{10}$	$9.36\cdot10^9$	$4.68\cdot10^9$	$2.34{:}10^9$	$4.68\cdot10^8$	$4.68\cdot10^7$	$4.82\cdot10^6$
30.00	29.03	$7.46\cdot10^{11}$	$2.99\cdot10^{11}$	$1.49\cdot10^{11}$	$7.46\cdot10^{10}$	$1.49\cdot10^{10}$	$1.49\cdot10^9$	$1.54\cdot10^8$

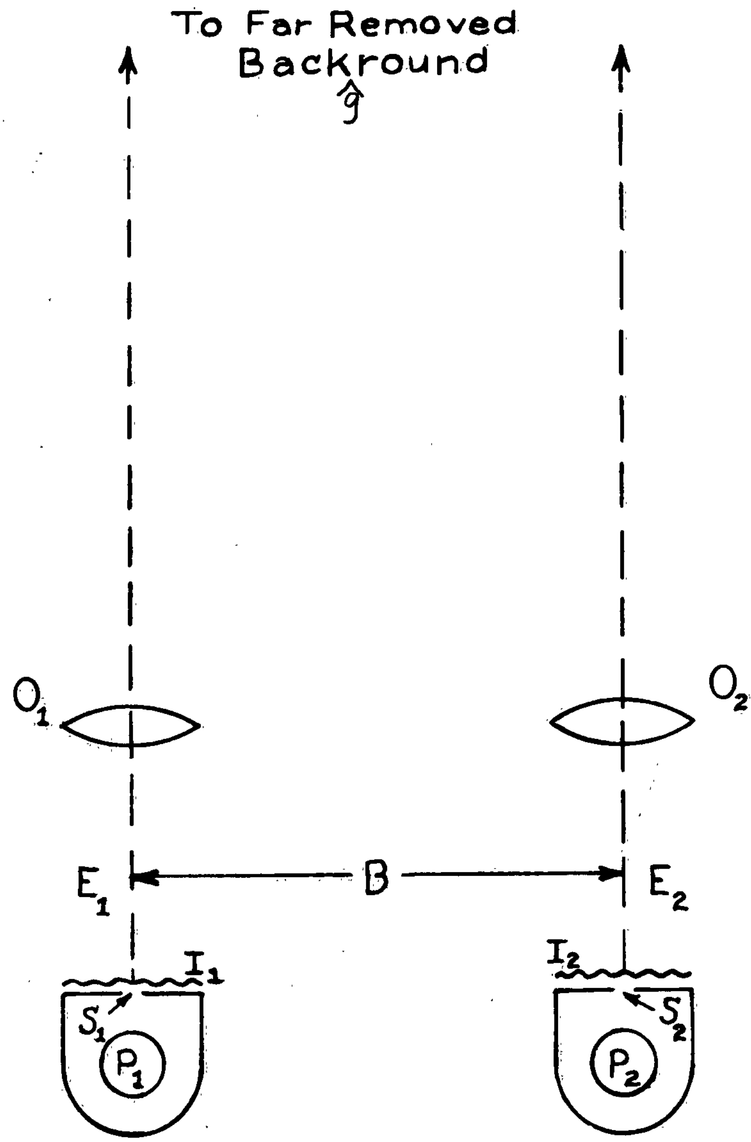

Figure 1. Mode of operation of the automatic optical range-finder.

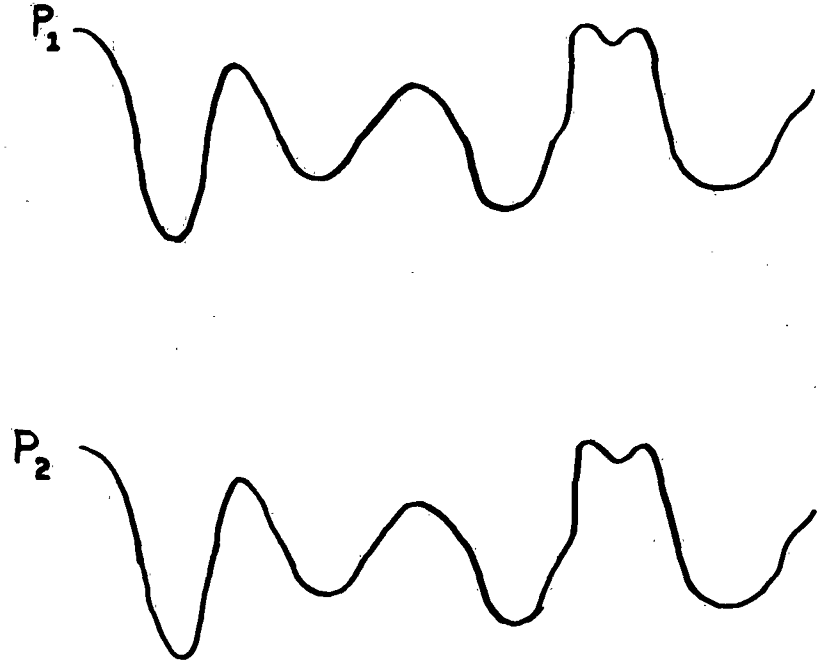

Figure 2. Output of the two photocells when infinite far background is scanned.

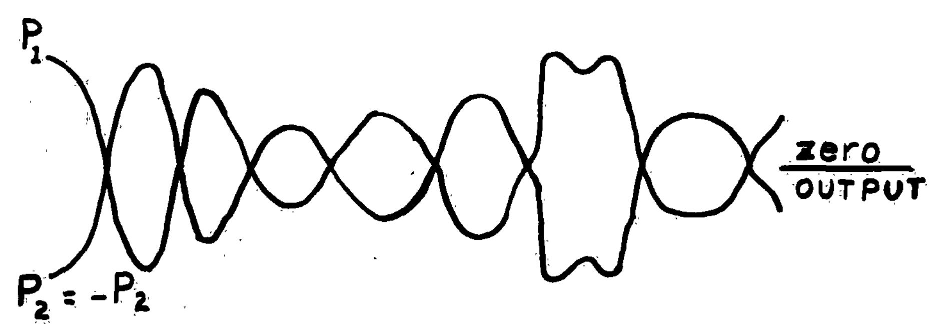

Figure 3. Compensation of photocell output to zero when infinite far background is scanned.

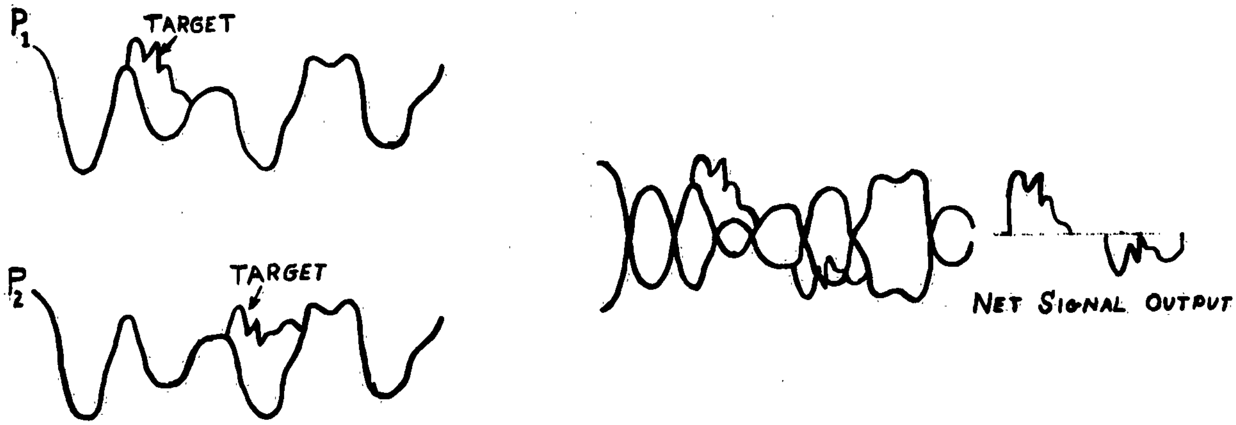

Figure 4. Target in finite distance produces net signal in compensated photocell output.

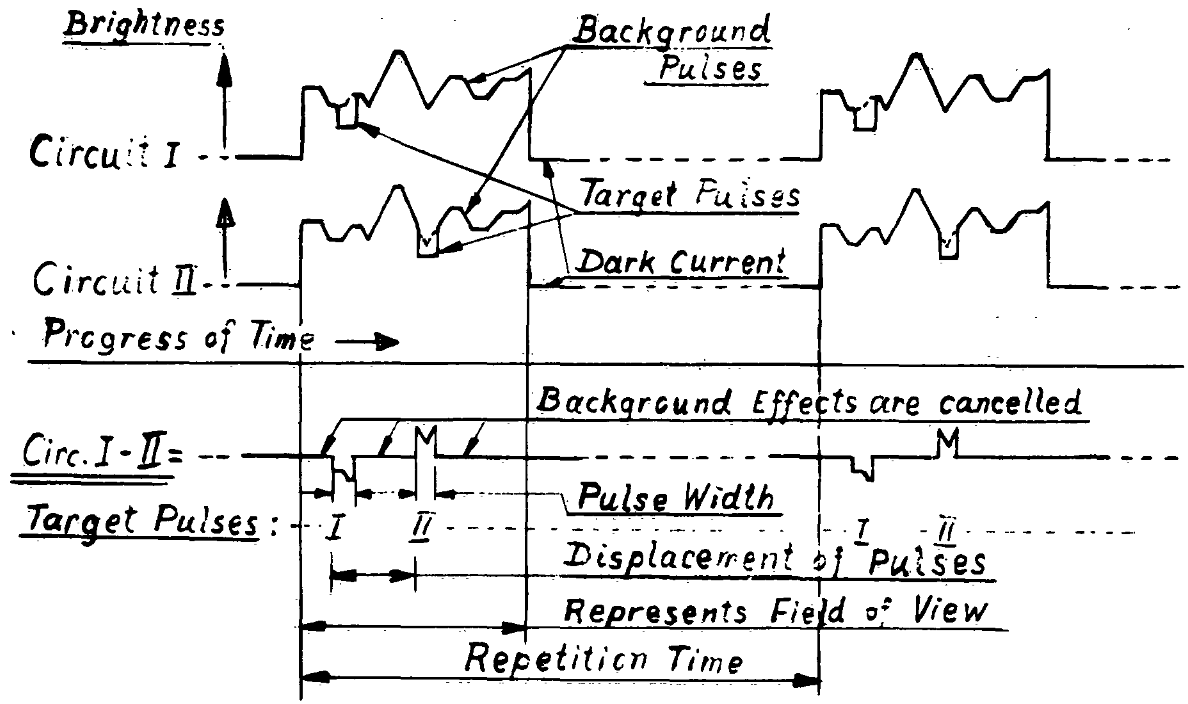

Figure 5. Detailed explanation of occurrence of net pulses when target is in finite distance.

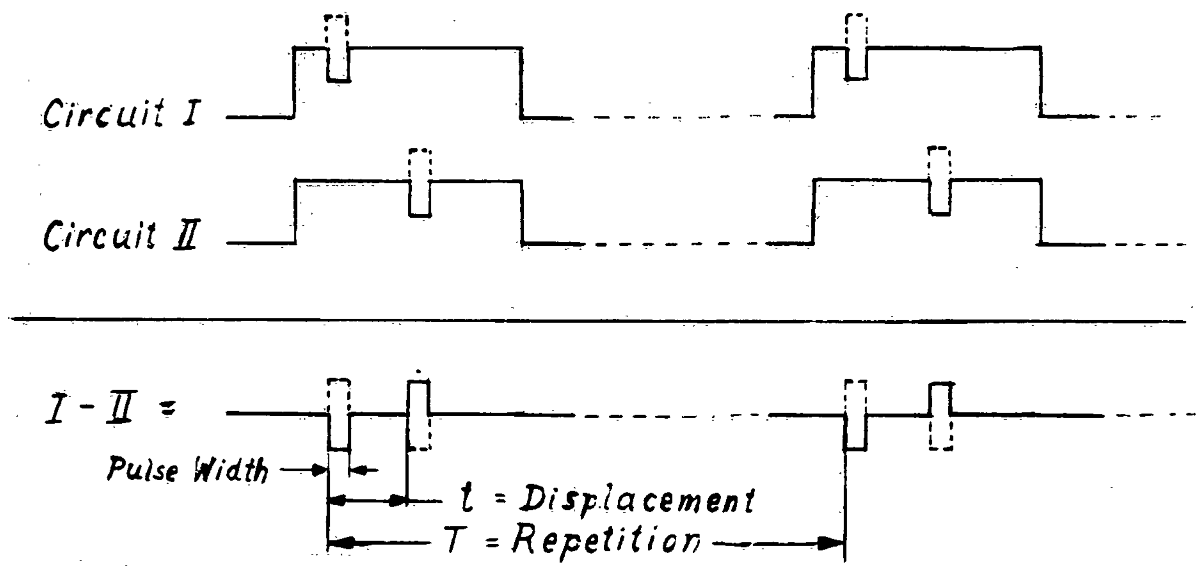

Figure 6. Small target produces two separated net pulses.

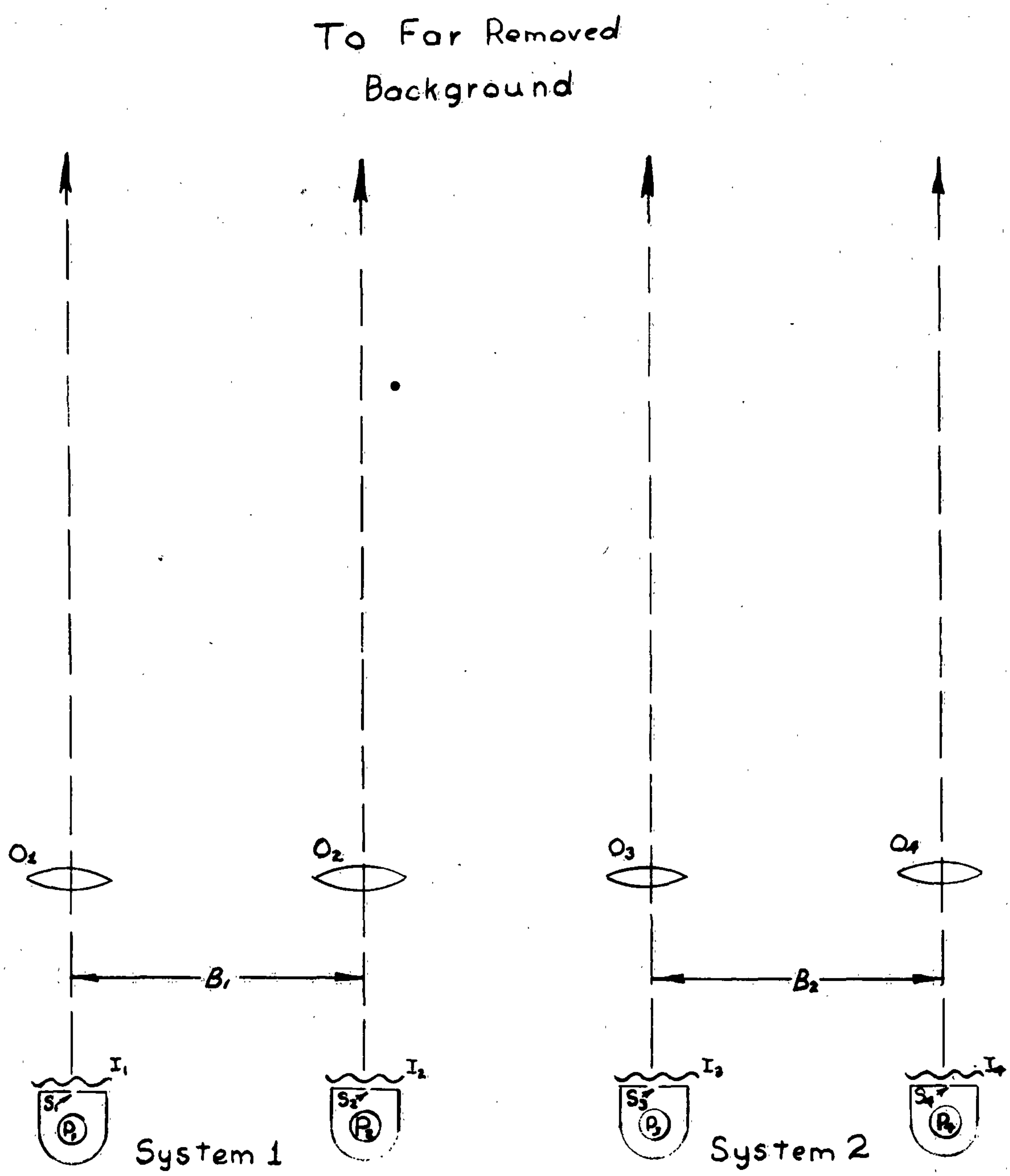

Figure 7. Mode of operation of a double range-finder system.

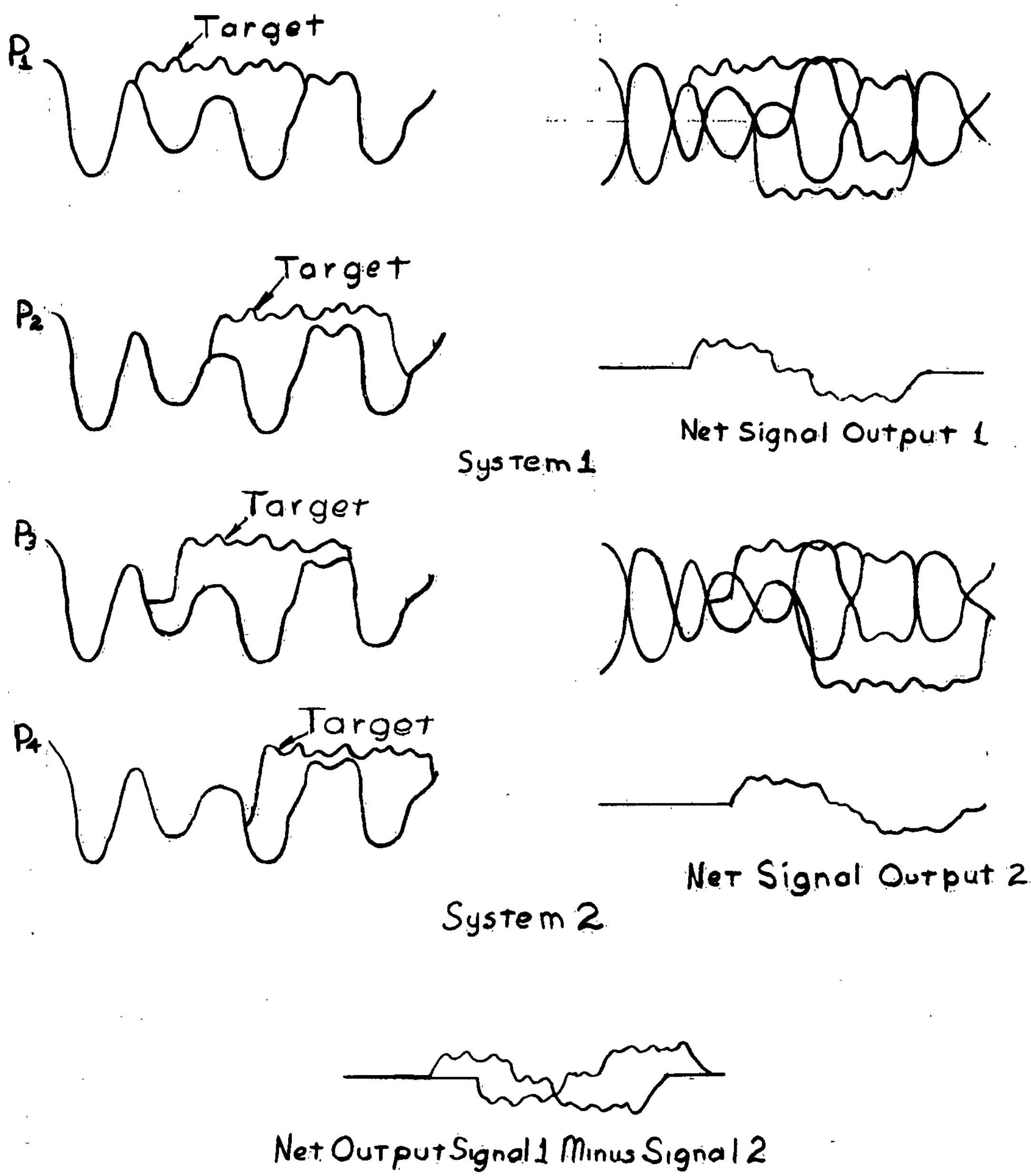

Figure 8. Net signal produced by a double range-finder system.

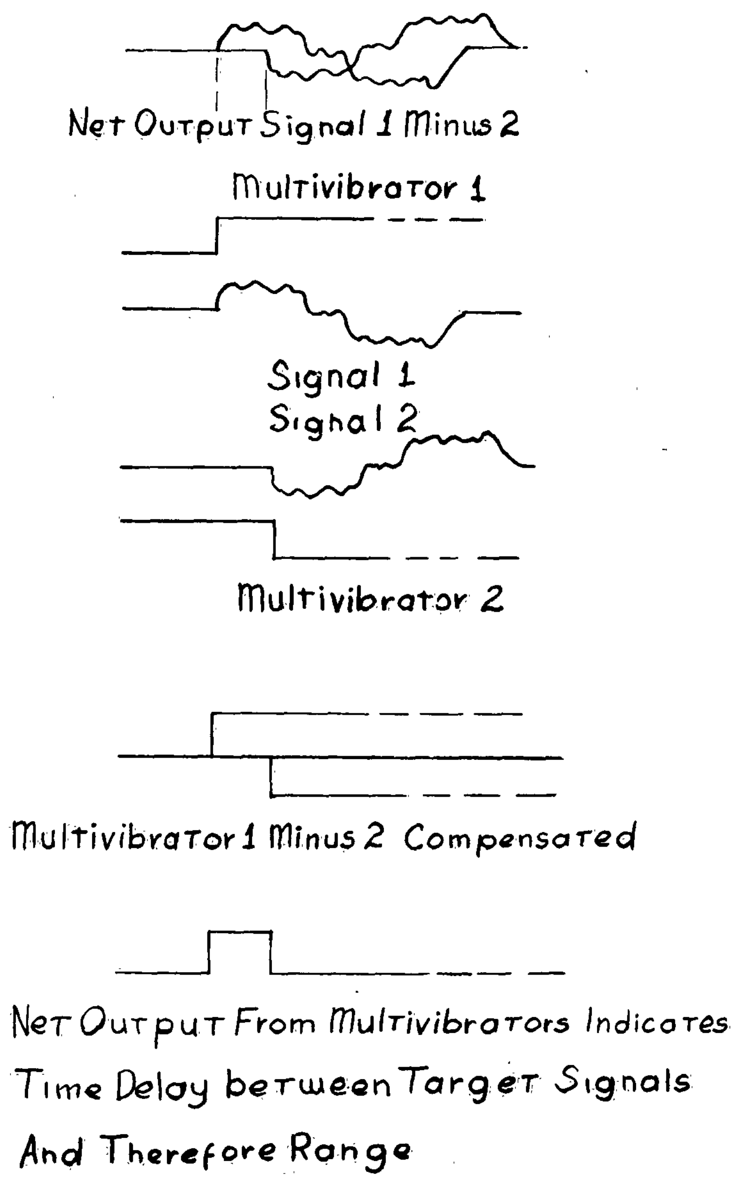

Figure 9. Extended target produces two separate net signals and compensated output in double range-finder system.

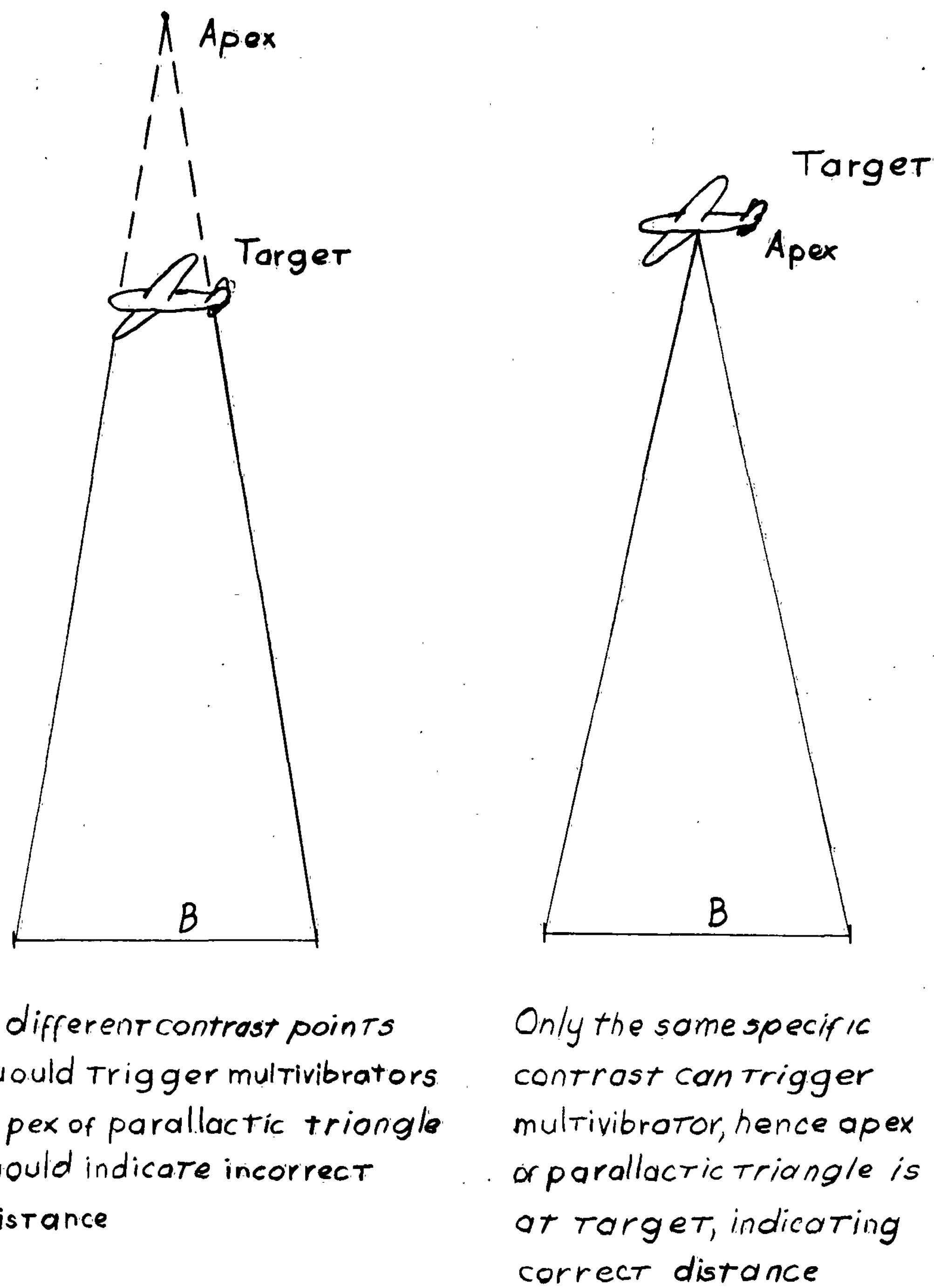

Figure 10. Parallactic triangle has its apex at the target.

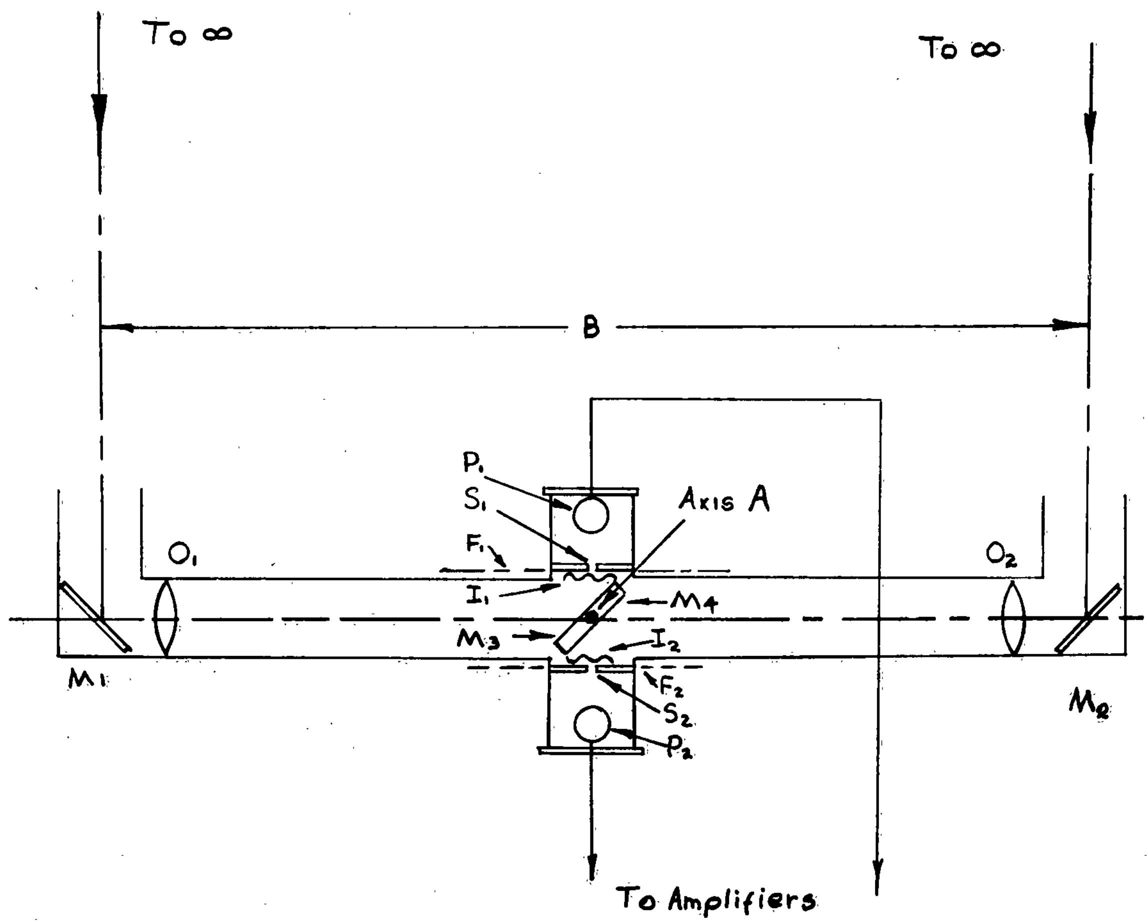

Figure 11. Construction of range-finder system when rotating double mirror is employed for scanning.

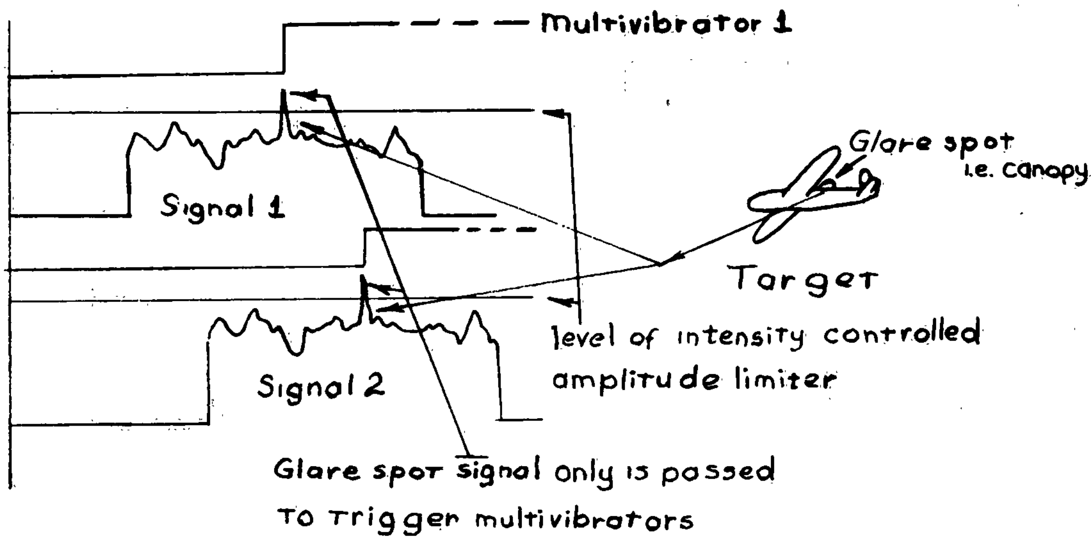

Figure 12. Production of rectangular pulses from net target pulses in the double range-finder system.

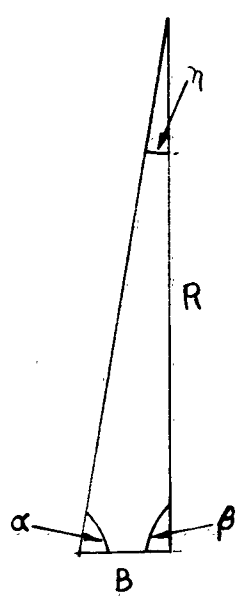

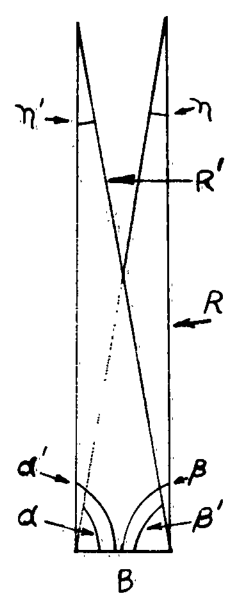

Figure 13. Parallactic triangle.

Figure 14. Relation of errors in the parallactic triangle.

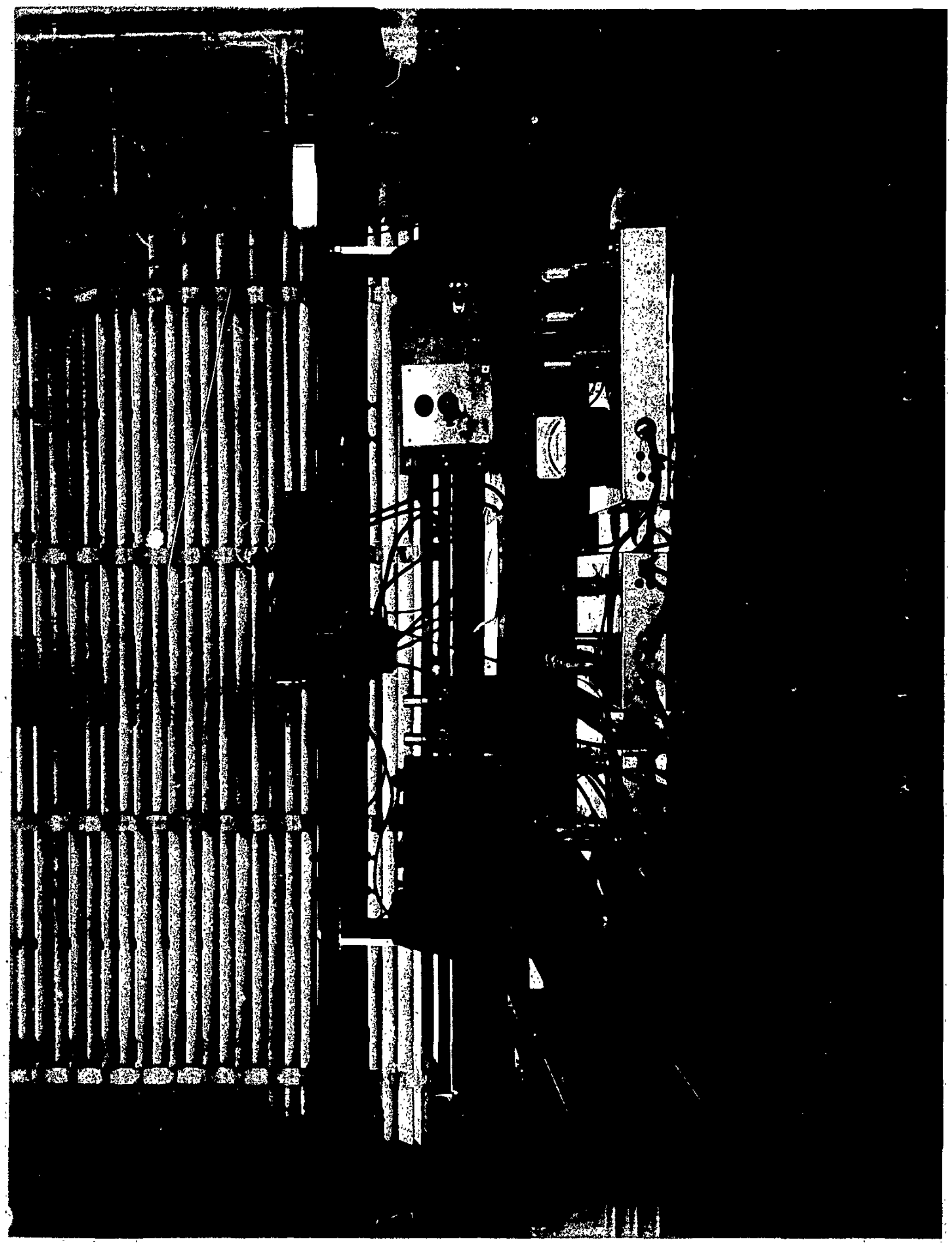

Figure 15. Working model of the range-finder.

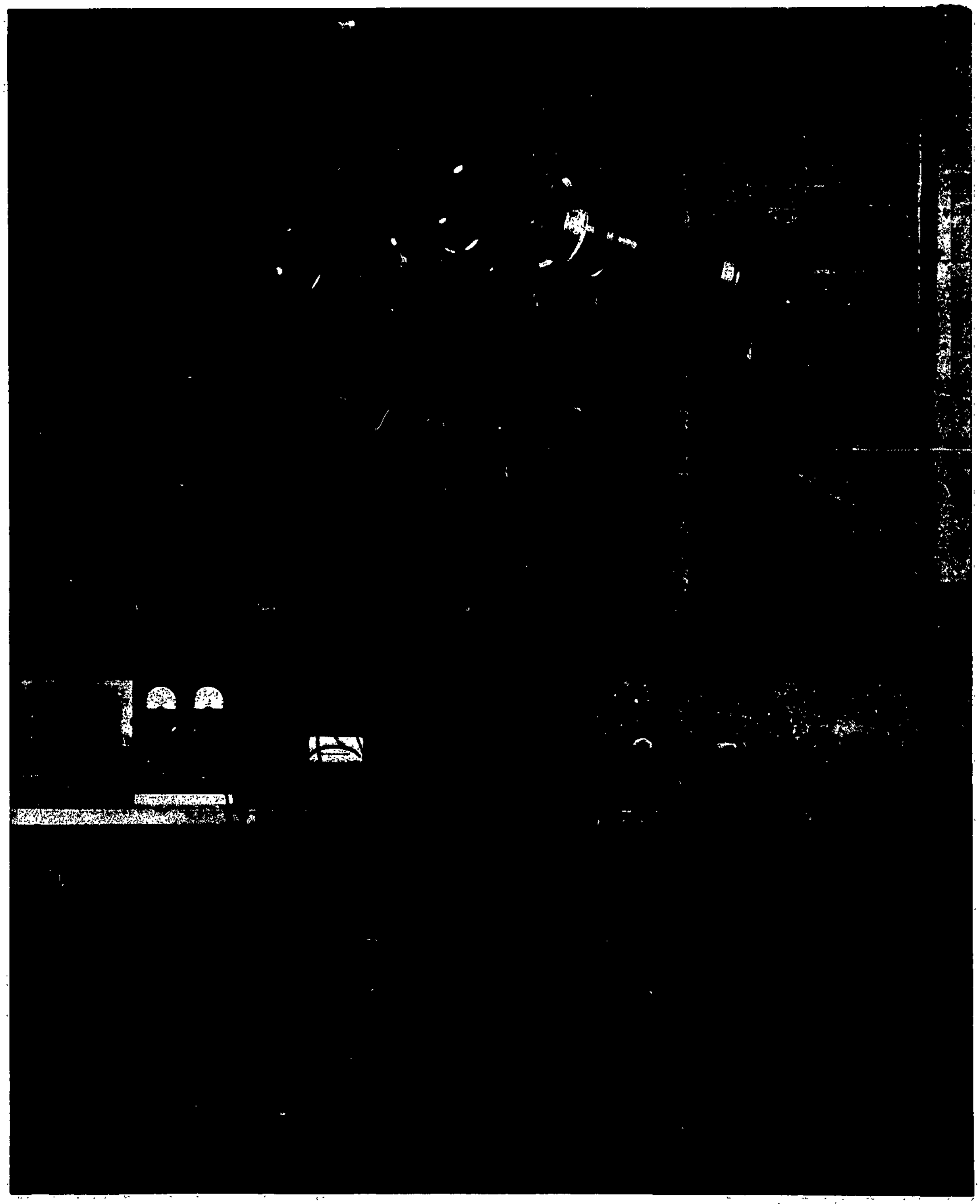

Figure 16. Parallactic photometer.

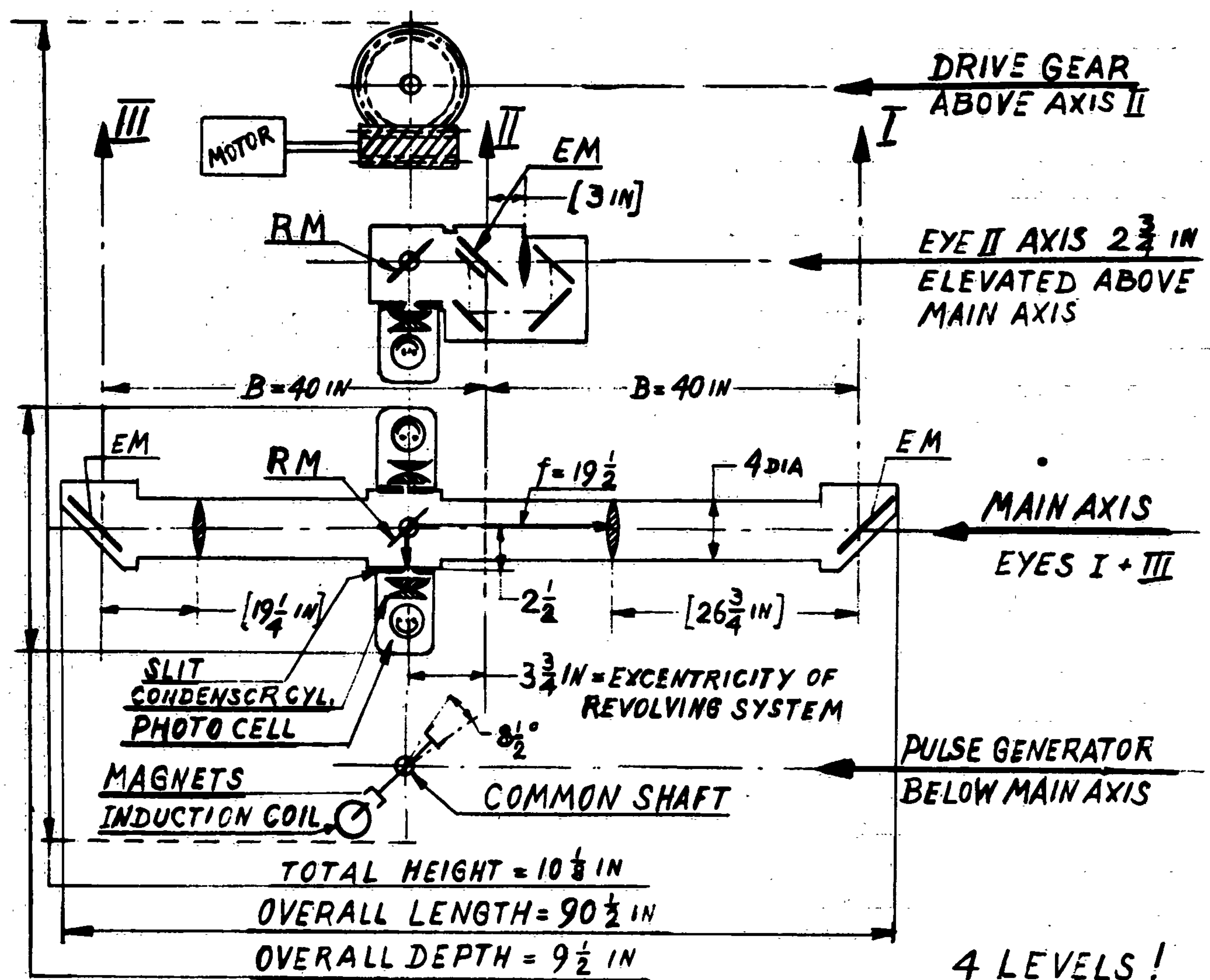

Figure 17. Sketch of the range-finder design

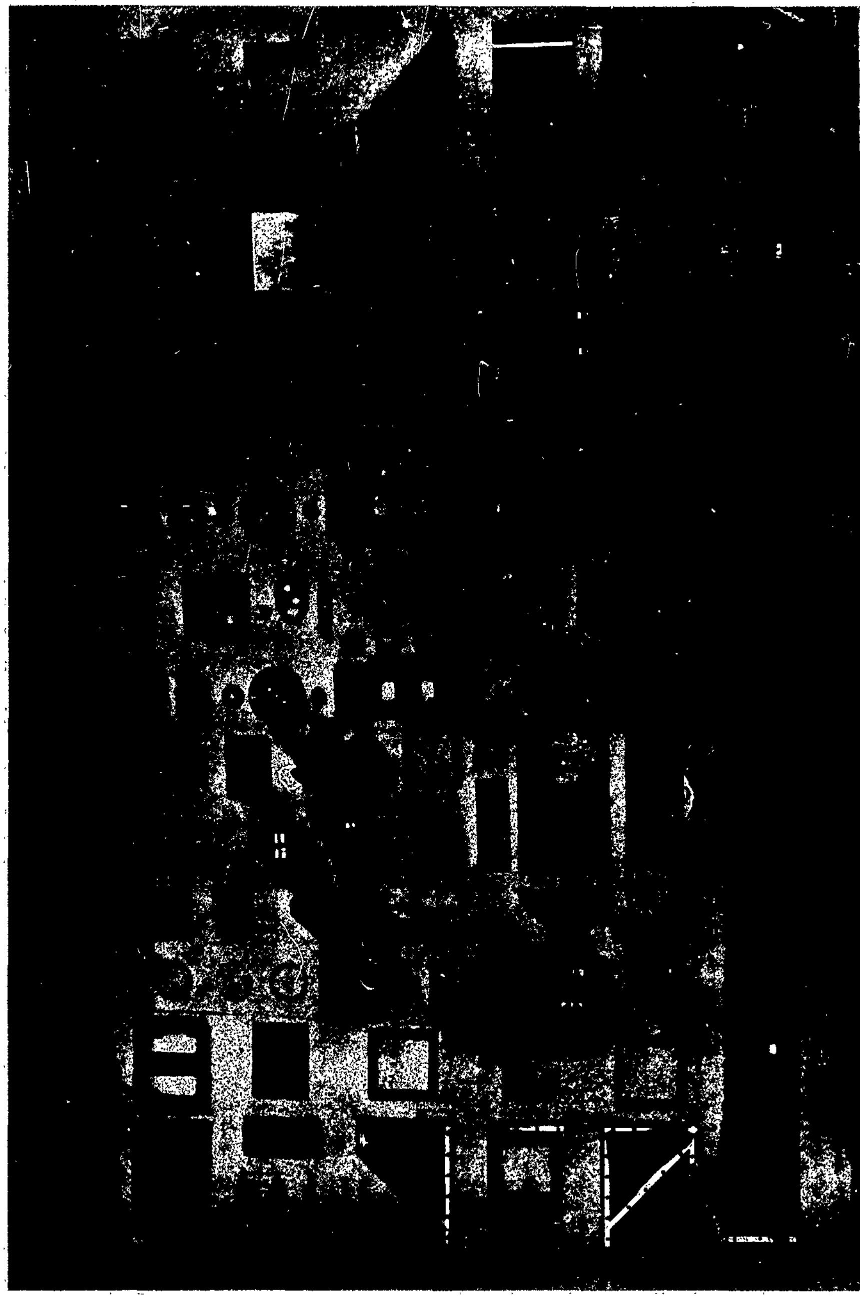

Figure 18. Parts of the model disassembled.

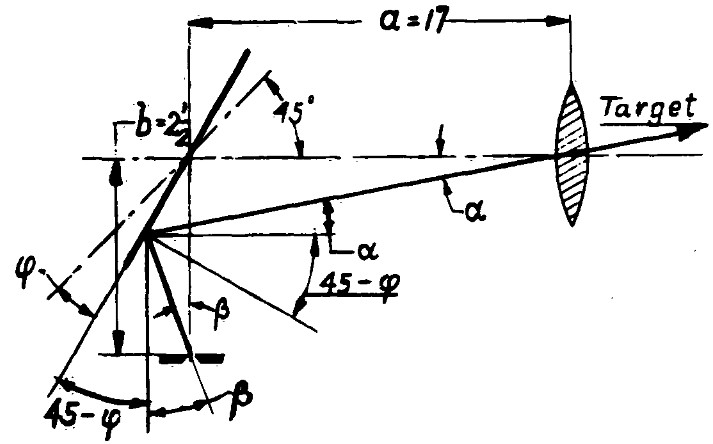

From Fig. 10 the following angular relations can be derived:

$$90^\circ - (45^\circ - \varphi + \beta) = 45^\circ - \varphi + \alpha \; : \; \varphi = \frac{\alpha + \beta}{2}$$

for small angles α ($\varphi \approx 45^\circ$):

$$\left.\begin{aligned} a \times \alpha &= b \times \beta \\ 17 \times \alpha &= 2{,}5 \times \beta \end{aligned}\right\} \quad \frac{\beta}{\alpha} = \frac{17}{2{,}5} = 6{,}8$$

Figure 19. Angular considerations.

(30)

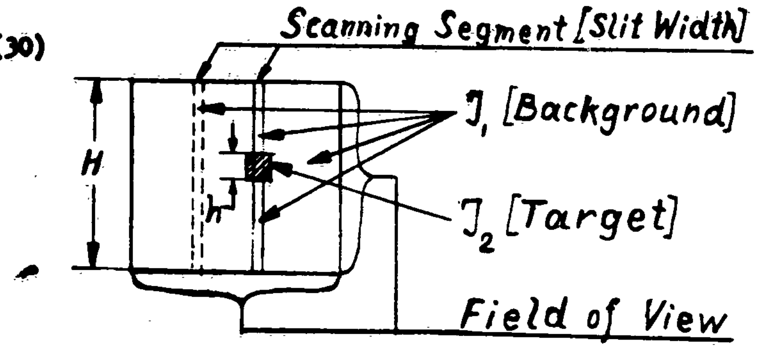

$$\delta = \frac{h}{H} = \frac{h_T^{[ft]}}{.75^{IN}} \times \frac{19.5^{IN}}{D^{ft}} = 26\frac{h_T^{ft}}{D^{ft}}$$

(see No. 24)

Wherein: h_T = Height of Target
D = Range
H = Length of Slit
h = Height of Image of Target

Figure 20. Explanation of reduction of measured contrast.

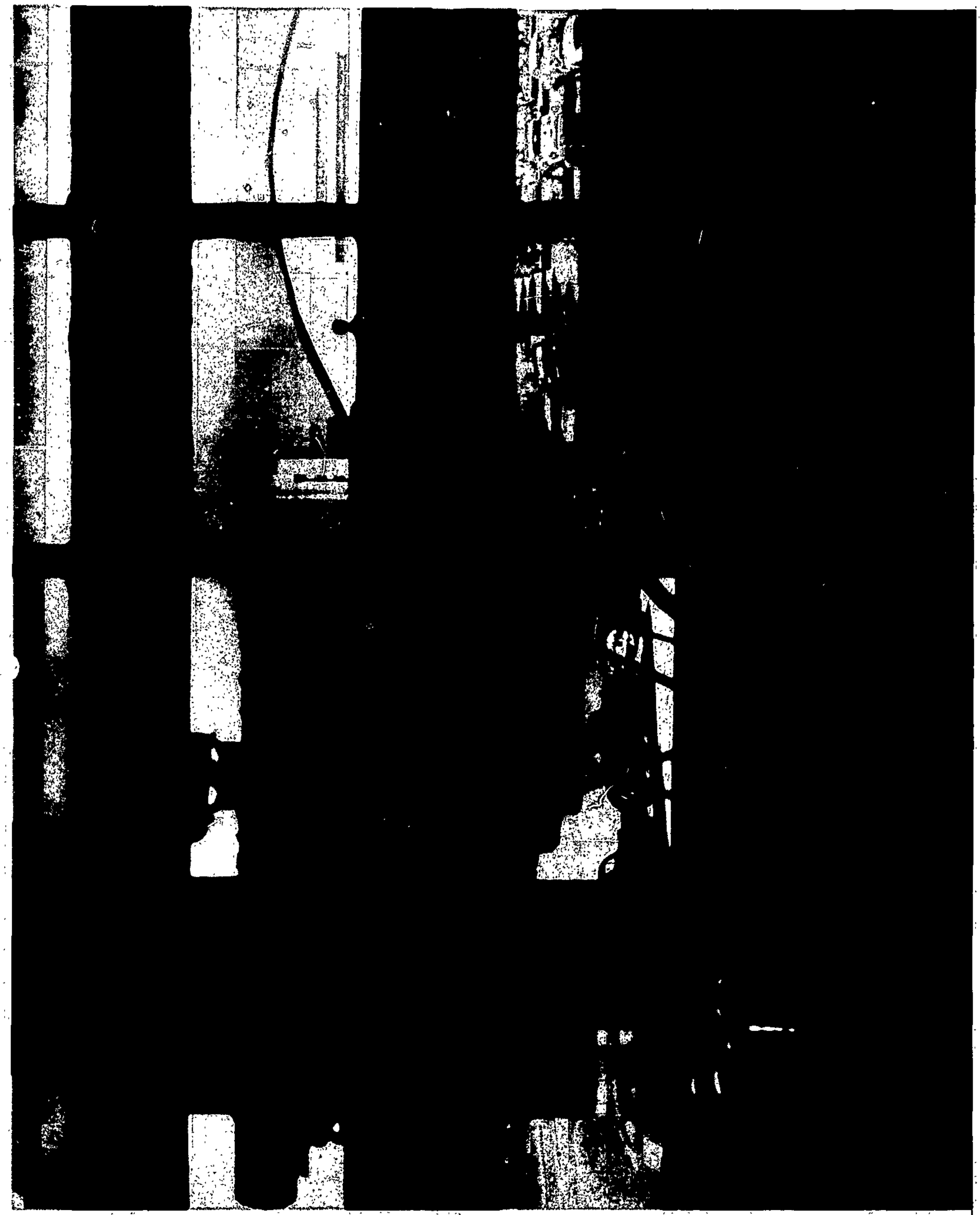

Figure 21. Arrows point to actual targets whose distances were measured.

Aeronautical Research Laboratories, Wright- Patterson AFB, O. AUTOMATIC OPTICAL RANGE FINDER by Werner Rambauske, Hubert Kuesters. February 1963. 39 p. incl. illus. (Project 7072; Task 70827) (ARL 63-48)
Unclassified Report

The different possible conventional methods usable for passive electronic range finding are analyzed. A new method is suggested, having considerable advantages over these. A working model to demonstrate this new method was designed and built for evaluation of experimental data and detailed

(over)

UNCLASSIFIED

UNCLASSIFIED

descriptions are added to the report.

UNCLASSIFIED

UNCLASSIFIED

Aeronautical Research Laboratories, Wright- Patterson AFB, O. AUTOMATIC OPTICAL RANGE FINDER by Werner Rambauske, Hubert Kuesters. February 1963. 39 p. incl. illus. (Project 7072; Task 70827) (ARL 63-48)
Unclassified Report

The different possible conventional methods usable for passive electronic range finding are analyzed. A new method is suggested, having considerable advantages over these. A working model to demonstrate this new method was designed and built for evaluation of experimental data and detailed

(over)

UNCLASSIFIED

UNCLASSIFIED

descriptions are added to the report.

UNCLASSIFIED

UNCLASSIFIED